

Comparison of Instantaneous Frequency Scaling from Rain Attenuation and Optical Disdrometer Measurements at K/Q bands

James Nessel, NASA Glenn Research Center, 21000 Brookpark Rd. MS 54-1,
Cleveland, OH 44135, +1 216-433-2546, james.a.nessel@nasa.gov

Michael Zemba, NASA Glenn Research Center, 21000 Brookpark Rd. MS 54-1,
Cleveland, OH 44135, +1 216-433-5357, michael.j.zemba@nasa.gov

Lorenzo Luini, Politecnico di Milano, Via Ponzio 34/5, 20133 - Milano,
+39 02-23993693, lorenzo.luini@polimi.it

Carlo Riva, Politecnico di Milano, Via Ponzio 34/5, 20133 - Milano,
+39 02-23993659, carlo.riva@polimi.it

Abstract

Rain attenuation is strongly dependent on the rain rate, but also on the rain drop size distribution (DSD). Typically, models utilize an average drop size distribution, such as those developed by Laws and Parsons, or Marshall and Palmer. However, individual rain events may possess drop size distributions which could be significantly different from the average and will impact, for example, fade mitigation techniques which utilize channel performance estimates from a signal at a different frequency. Therefore, a good understanding of the characteristics and variability of the raindrop size distribution is extremely important in predicting rain attenuation and instantaneous frequency scaling parameters on an event-to-event basis. Since June 2014, NASA Glenn Research Center (GRC) and the Politecnico di Milano (POLIMI) have measured the attenuation due to rain in Milan, Italy, on the 20/40 GHz beacon signal broadcast from the Alphasat TDP#5 Aldo Paraboni Q/V-band Payload. Concomitant with these measurements are the measurements of drop size distribution and rain rate utilizing a Thies Clima laser precipitation monitor (disdrometer). In this paper, we discuss the comparison of the predicted rain attenuation at 20 and 40 GHz derived from the drop size distribution data with the measured rain attenuation. The results are compared on statistical and real-time bases. We will investigate the performance of the rain attenuation model, instantaneous frequency scaling, and the distribution of the scaling factor. Further, seasonal rain characteristics will be analysed.

I. Introduction

Typically, rain rate statistics for a given site are measured by tipping bucket rain gauges. These measurement devices are cost effective and sufficient for modelling long term rain attenuation and frequency scaling statistics. However, for estimates of instantaneous rain attenuation and instantaneous frequency scaling parameters, knowledge of the characteristics and variability of the raindrop size distribution is extremely important, as the specific attenuation experienced by electromagnetic waves propagation through rain is dependent not only on the rain rate, but on the variability of the drop size distribution (DSD) of the rain, as well [1]. This becomes particularly important as communications systems move into the millimeter wave, or when, fade mitigation techniques employing, for example, uplink power control, are implemented based on measurements of a lower frequency downlink signal.

Since June 2014, NASA Glenn Research Center (GRC) and the Politecnico di Milano (POLIMI) have measured the attenuation due to rain in Milan, Italy, on the 20/40 GHz beacon signal broadcast from the Alphasat TDP#5 Aldo Paraboni Q/V-band Payload. Concomitant with these measurements are the measurements of drop size distribution and rain rate utilizing a Thies Clima laser precipitation monitor

(disdrometer). In this paper, we discuss the comparison of the predicted rain attenuation at 20 and 40 GHz derived from the drop size distribution data with the measured rain attenuation. The results are compared on statistical and real-time bases. We will investigate the performance of the rain attenuation model, instantaneous frequency scaling, and the distribution of the scaling factor. Further, seasonal rain characteristics will be analyzed.

II. Experiment Setup

A propagation campaign monitoring the attenuation due to rain at 20/40 GHz utilizing the Alphasat Aldo Paraboni Q/V-band Payload has been underway since June 2014 in Milan, Italy, as a joint effort between NASA Glenn Research Center (GRC) and the Politecnico di Milano (POLIMI). The experimental setup is installed on the rooftop of the Dipartimento di Elettronica, Informazione e Bioingegneria (DEIB) building on the POLIMI campus. The measuring instruments include a K-band and Q-band beacon receiver, a weather station monitoring temperature, pressure, humidity and wind speed/direction, a tipping bucket, and an optical disdrometer, as shown in the photograph of Figure 1. Here we discuss in more detail the performance and operations of the beacon receivers and optical disdrometer, which are the focus of this paper.

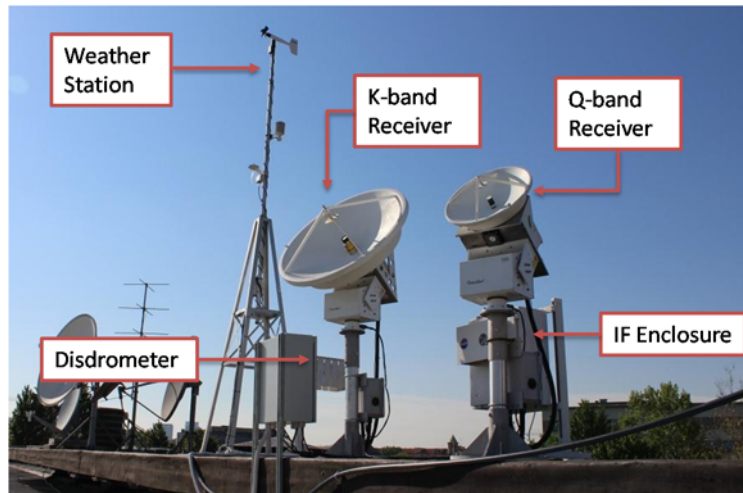


Figure 1. Photograph of experiment setup at POLIMI campus.

Alphasat Beacon Receiver

The Alphasat beacon receiver, developed at NASA GRC, consists of a 1.2m K-band and a 0.6m Q-band Cassegrain reflector with equivalent antenna beamwidths of 0.9 deg. A more detailed description of the beacon receiver hardware can be found in [2]. Table I provides a summary of the relevant receiver system parameters. Essentially, both the K and Q-band signals broadcast from the Alphasat satellite are actively tracked, received, and downconverted to a common final IF of 455 kHz. All downconversion stages are coherently locked to the same common ultra-stable 10 MHz reference oscillator. A block diagram of the coherent receivers is shown in Figure 2. The IF signal is digitized and the software utilizes a novel modified Quinn-Fernandes-Nessel frequency estimation routine to record the frequency and power level of the signals [3]. A measurement bandwidth of approximately 8.5 Hz is employed to record the data at a measurement rate of 8 Hz, which are then averaged each second to generate 1 Hz measurement data simultaneously. This approach allows the receivers to maintain a dynamic range of approximately 40 dB.

Table I. Performance specifications for the K/Q-band beacon receivers.

Receiver Parameters	Performance Spec.
Center Frequency	19.701 GHz (K-band) 39.402 GHz (Q-band)
Antenna Gain	45.6 dBi
System Noise Temperature	504 K (K-band) 720 K (Q-band)
ADC Sampling Rate	1.111 MHz
No. of Samples	2^{17}
Measurement Bandwidth	8.5 Hz
Measurement Rates	8 Hz/1 Hz(averaged)
Dynamic Range	38 dB (K-band) 40 dB (Q-band)

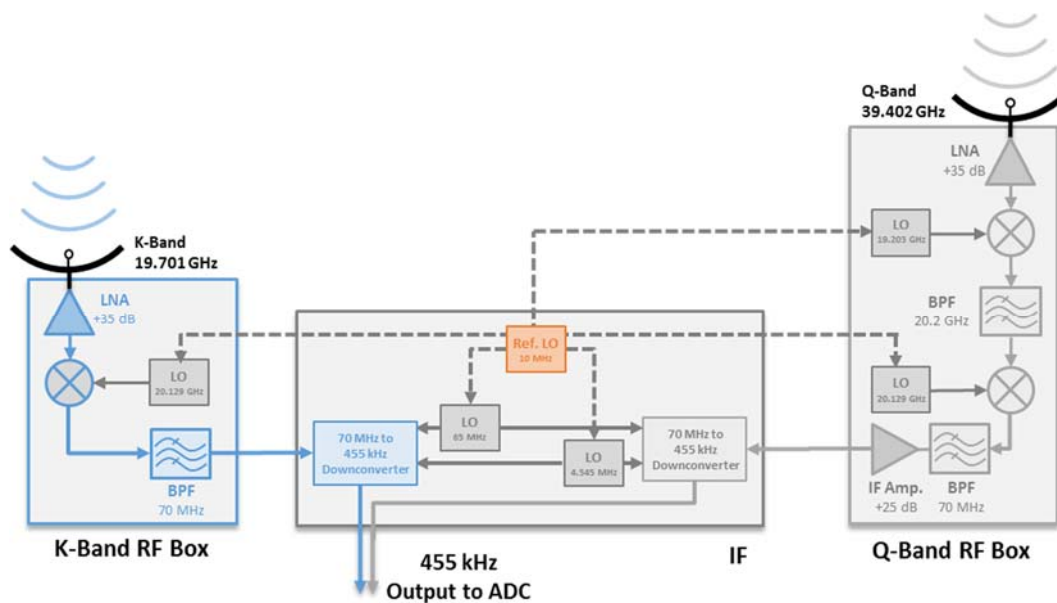


Figure 2. Block diagram of K-band and Q-band beacon receivers.

Thies Clima Laser Precipitation Monitor

The Thies Clima Laser Precipitation Monitor (disdrometer) is located adjacent to the weather station on the DEIB rooftop, as indicated in Figure 1. It utilizes an infrared laser diode to generate a 785 nm parallel light beam covering a 4560 mm² area swath, as depicted in Figure 3 [4]. A photodiode on the receive end of the light beam monitors the reduction in receive signal strength as precipitating particles cross the beam. From this measurement, details on the particle size and fall velocity can be derived from the magnitude and duration of the signal attenuation, respectively. An on-board digital signal processor classifies the type, intensity, quantity, and particle spectrum of precipitation over 1 minute intervals. The particle spectrum is classified into 22 diameter bins from 0.125 mm to 8 mm and 20 velocity bins from 0 to 10 m/s with non-uniform bin widths, as described in Table II. The on-board processor also derives estimates of the rain rate from the drop size distribution (DSD) data.

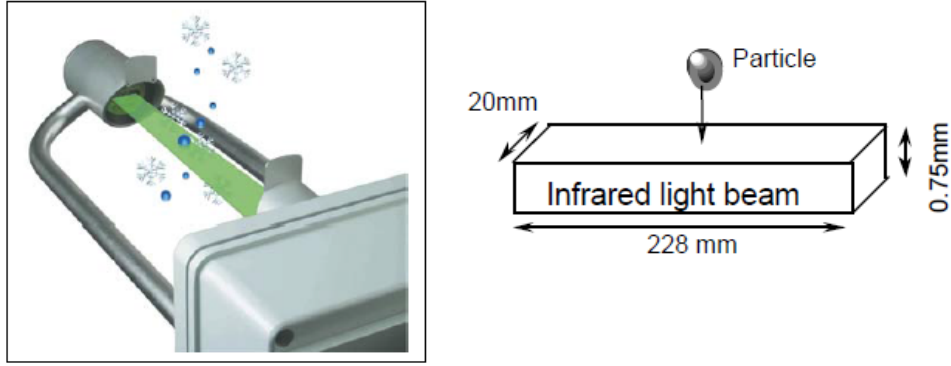


Figure 3. Measurement of a precipitating particle [4].

Table II. Disdrometer class binning of diameter and speed [4].

Particle diameter class			Particle speed class		
Class	Diameter [mm]	Class width [mm]	Class	Speed [m/s]	Class width [m/s]
1	≥ 0.125	0.125	1	≥ 0.000	0.200
2	≥ 0.250	0.125	2	≥ 0.200	0.200
3	≥ 0.375	0.125	3	≥ 0.400	0.200
4	≥ 0.500	0.250	4	≥ 0.600	0.200
5	≥ 0.750	0.250	5	≥ 0.800	0.200
6	≥ 1.000	0.250	6	≥ 1.000	0.400
7	≥ 1.250	0.250	7	≥ 1.400	0.400
8	≥ 1.500	0.250	8	≥ 1.800	0.400
9	≥ 1.750	0.250	9	≥ 2.200	0.400
10	≥ 2.000	0.500	10	≥ 2.600	0.400
11	≥ 2.500	0.500	11	≥ 3.000	0.400
12	≥ 3.000	0.500	12	≥ 3.400	0.800
13	≥ 3.500	0.500	13	≥ 4.200	0.800
14	≥ 4.000	0.500	14	≥ 5.000	0.800
15	≥ 4.500	0.500	15	≥ 5.800	0.800
16	≥ 5.000	0.500	16	≥ 6.600	0.800
17	≥ 5.500	0.500	17	≥ 7.400	0.800
18	≥ 6.000	0.500	18	≥ 8.200	0.800
19	≥ 6.500	0.500	19	≥ 9.000	1.000
20	≥ 7.000	0.500	20	≥ 10.000	10.000
21	≥ 7.500	0.500			
22	≥ 8.000	∞			

III. Specific Attenuation from DSD Data

To determine the specific rain attenuation at 20 and 40 GHz from the disdrometer data, the following procedure was implemented. The specific attenuation (γ) is a function of the wavelength (λ , in m), forward scattering coefficient ($Re\{S(0)\}$), and drop density distribution ($N(D)$, in $m^{-3}mm^{-1}$) as [5],

$$\gamma = 4.343 \times 10^3 \frac{\lambda^2}{\pi} \sum Re\{S(0)\}N(D)\Delta D \quad (1)$$

where ΔD is the drop size interval (in mm). The forward scattering coefficient, which is also dependent on frequency, radius of the rain drop, and temperature, was calculated utilizing the Mie scattering model [6], which necessarily implies that the rain drops are spherical in shape, which was a simplifying assumption taken at this stage to permit a simplified analytical calculation of $S(0)$. The complex refractive index of water at 20 and 40 GHz at an average temperature of 20°C was taken from [5]. To calculate the drop density distribution from the binned DSD data, the following relation was used [7].

$$N(D_i) = \frac{n_i(D_i) \times 10^6}{v(D_i) \times S \times T \times \Delta D_i} \quad (2)$$

where the subscript, i , denotes the discretized i th bin from the disdrometer data, $n_i(D_i)$ is the number of drops with mean diameter D_i , $v(D_i)$ is the terminal velocity in still air (in m/s), S is the sample area for the Thies Clima Disdrometer (4560 mm²), T is the integration time (60 sec), and ΔD_i is the bin width of each drop size class (in mm), as indicated in Table II. All of these parameters are directly available from the recorded DSD data and the specifications of the disdrometer hardware, except for the terminal velocity, which was modelled using the widely accepted analytical fit of measured data by Gunn and Kinzer, given by [8-10].

$$v(D_i) = 9.65 - 10.3e^{-0.6D_i} \quad (3)$$

IV. Analysis Results

Data taken during the measurement period of August 2014 to August 2015 were filtered to isolate rain events only when the disdrometer recorded rainfall over the site. Rain events in which the disdrometer was not operational or rain that occurred along the path, but was not detected directly over the site were removed. Due to the lack of a radiometer, for each rain event, pre- and post-rain event levels were averaged in an attempt to isolate the excess attenuation due to rain only, though attenuation due to clouds may still introduce a bias to the attenuation measurement, particularly at the higher 40 GHz frequency. In all, 100 rain days were identified and analysed in both an instantaneous and statistical basis. One minute averages were used to compare the results of the disdrometer DSD data and the rain attenuation data.

Instantaneous Frequency Scaling

We first analyze the accuracy of the use of drop size distribution data as recorded from the This Clima Laser Precipitation Monitor to predict rain attenuation at 40 GHz from the 20 GHz data. A frequency scaling factor is derived from the DSD data and defined as the ratio of the specific attenuation at 40 GHz to the specific attenuation at 20 GHz, as provided in Equation (1). As such, the scaling factor is updated in 1-min intervals and used to predict 40 GHz rain attenuation from the 20 GHz rain attenuation time series. Figures 4 and 5 show representative time series for a relatively low rain rate (i.e., 1-10 mm/hr) and a high rain rate (i.e., >40 mm/hr), in which the DSD data is used to scale the measured rain attenuation at 20 GHz to the measured rain attenuation at 40 GHz. In both cases, the scaling factor predicted using the Mie scattering model and the DSD data do a good job in predicting the 40 GHz rain attenuation levels, to within a mean error of 0.63 dB and 1.16 dB, for the low and high rain rate cases, respectively, where the largest error in the high rain rate case is due to the fact that the maximum dynamic range of the beacon receiver is 40 dB, but use of the DSD data predicted a maximum rain attenuation of almost 60 dB. Analysis of all recorded rain data from August 2014 – August 2015 indicate that the use of the DSD data to scale the 20 GHz rain attenuation to a predicted 40 GHz rain attenuation value agrees with the measured data to an average mean error of 0.86 dB and a root mean square error of 2.4 dB.

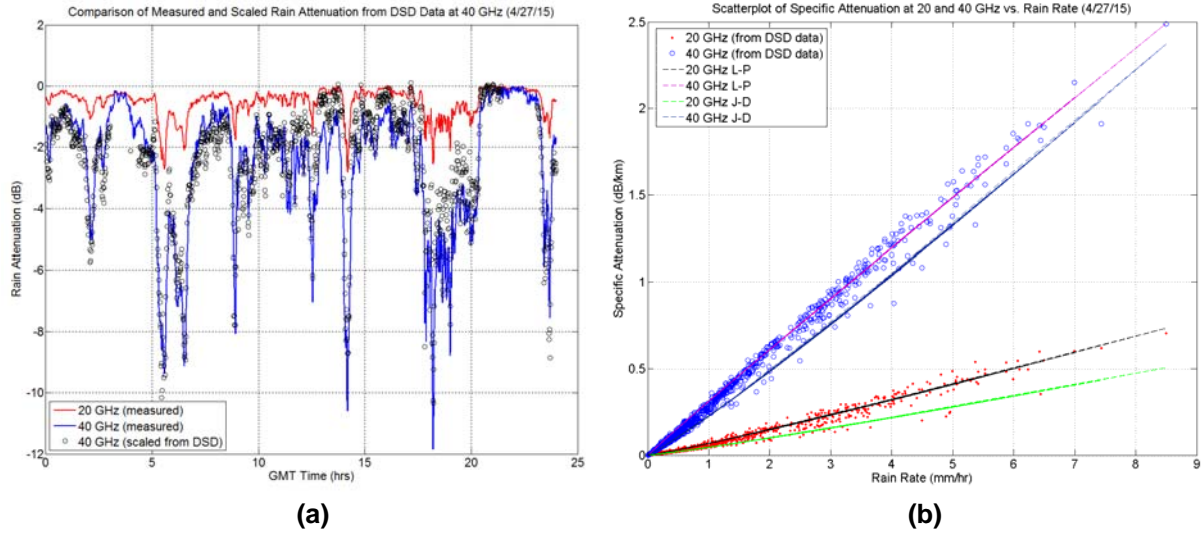


Figure 4. (a) Time series of rain attenuation data taken on April 27, 2015, comparing the measured to the predicted rain attenuation at 40 GHz derived by scaling the 20 GHz data with the measured DSD data. The rain rate for the day was in the range of 1-10 mm/hr. (b) Scatterplot of specific attenuation at 20 and 40 GHz derived from DSD data, compared with Laws-Parsons and Joss Drizzle distributions.

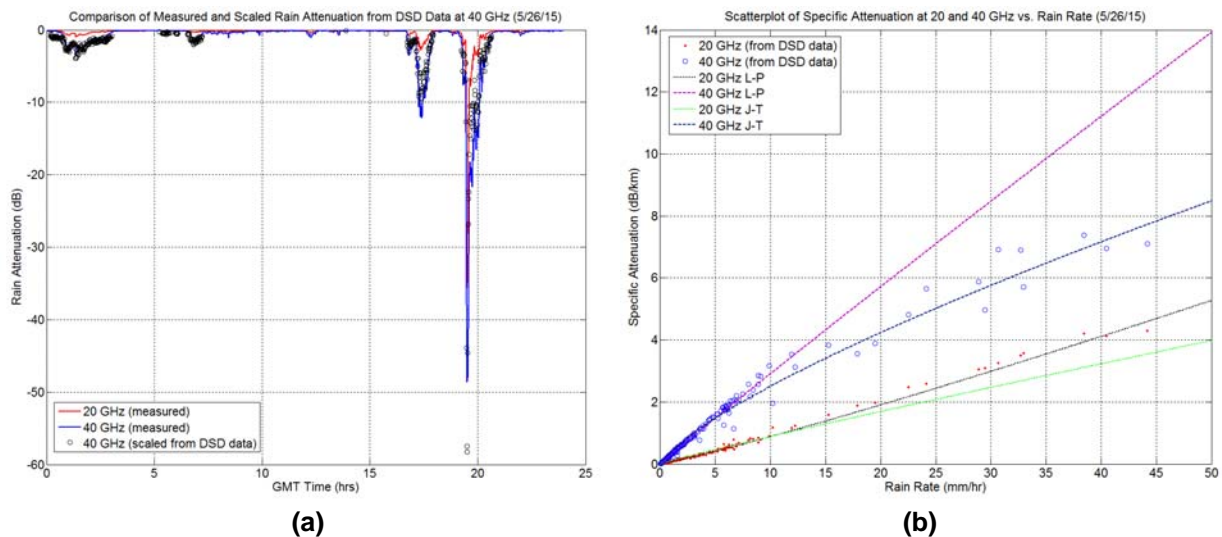


Figure 5. (a) Time series of rain attenuation data taken on May 26, 2015, comparing the measured to the predicted rain attenuation at 40 GHz derived by scaling the 20 GHz data with the measured DSD data. The rain rate for the day reached a maximum of 45 mm/hr. (b) Scatterplot of specific attenuation at 20 and 40 GHz derived from DSD data, compared with Laws-Parsons and Joss Thunderstorm distributions.

From the low rain rate data, we also observe that the rain drop size distribution tends to be bounded by the Laws-Parsons and the Joss Drizzle distribution, while for the high intensity event, albeit small amount of data have been recorded during such event, we show the rain data agrees within the bounds of the Laws-Parsons and Joss Thunderstorm distribution models for that day. Overall, for both sample events, the scatter plots point out that there might be also a marked variability in the DSD even within a single event, typically between the beginning of the event and its remainder.

Statistics of Frequency Scaling Factor

A comparison of the probability distribution of the frequency scaling factor derived from the point measurement of the disdrometer and the path measurement of rain attenuation from the beacon receivers was performed and shown in Figure 6. It is difficult to compare directly these two results since the drop size distribution measured over the receivers will not directly correspond to the drop size distribution along the entire path. However, it is interesting to observe from the comparison of these two distributions that the most probable scaling factors correspond to similar values between 4.5 – 5.5, with a much larger spread in the path measured data than in the point measured data, which is expected.

The rain drop size distributions were also analysed on a seasonal basis and the results are shown in Figure 7, compared to the standard Marshall-Palmer distribution [11]. The distribution, on average, tends to agree with the Marshall-Palmer distribution, with deviations towards higher rain drop diameters evident in the spring and summer months which appear to have an improved correlation with the Joss-Thunderstorm model, based on the limited one year of data collected to date. The rain drop size distribution in the wintertime agrees very well with the Marshall-Palmer distribution utilizing an average rain rate commensurate with the measured disdrometer rain rates during the winter months.

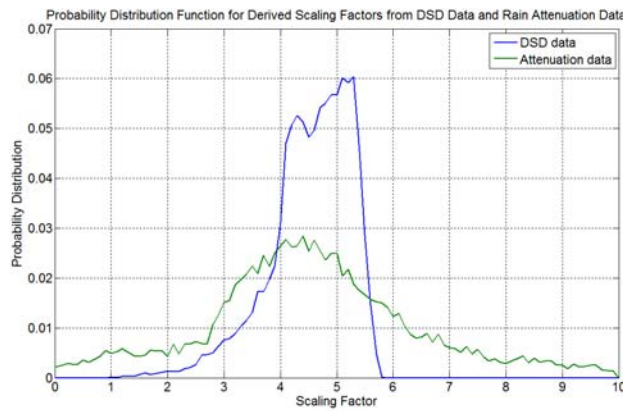


Figure 6. Probability distribution of scaling factor derived from DSD data and from attenuation data.

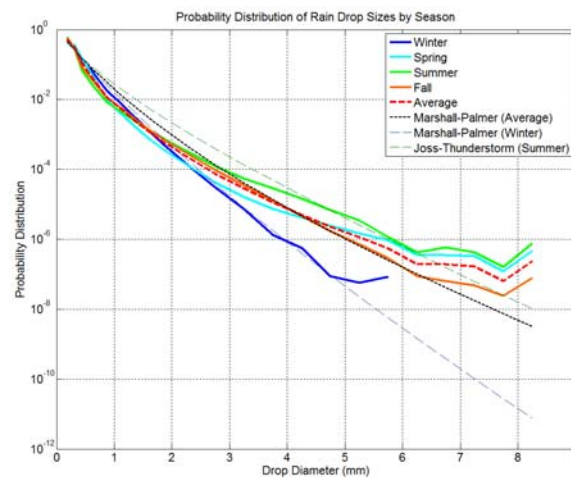


Figure 7. Probability distribution of rain drop sizes separated by season.

V. Conclusions

Herein we reported on the use of drop size distribution data to predict rain attenuation at 40 GHz utilizing the measured rain attenuation at 20 GHz. The DSD data was utilized to derive an instantaneous frequency scaling factor and the resulting 40 GHz predicted rain attenuation was compared with concomitant measured 40 GHz rain attenuation data. The comparison indicates that the use of the DSD data results in an average mean error of 0.86 dB, with a root mean square error of 2.4 dB. Preliminary analyses indicate that variability in the drop size distribution for a given day, or even within a given rain event, is present and could result in prediction errors when trying to implement fade mitigation techniques employing information from, for example, a beacon signal at a different frequency than the uplink or downlink signal. However, the analysis presented in this paper indicates that the use of a disdrometer at the ground station site could reduce uncertainties in prediction of rain attenuation, even though measurements produced by the disdrometer are point measurements in nature. Future work will investigate prediction error using the scaling factor as a function of the attenuation level, correlation between the scaling factor and the rain rate, and an in-depth analysis of the temporal variability of the drop size distribution both within a given rain event and across multiple rain events in a given day.

VI. References

- [1] H.Y. Lam, L. Luini, J. Din, C. Capsoni, A. D. Panagopoulos, "Investigation of Rain Attenuation in Equatorial Kuala Lumpur", *IEEE Antennas and Wireless Propagation Letters*, vol. 11, Page(s): 1002-1005, doi: 10.1109/LAWP.2012.2214371, 2012.
- [2] J. Nessel, J. Morse, M. Zemba, C. Riva, L. Luini, "Preliminary Results of the NASA Beacon Receiver for the Alphasat Aldo Paraboni TDP5 Propagation Experiment," 20th Ka and Broadband Communications Conference, Salerno, Italy, October 2014.
- [3] M. Zemba, J. Morse, J. Nessel, "Frequency Estimator Performance for a Software-based Beacon Receiver," *IEEE Antennas and Propagation Symposium*, July 2014, pp.1574-1575.
- [4] Thies Clima Laser Precipitation Monitor: Instructions for Use. Rev. 2.5. July 2011.
- [5] M. Sadiku, *Numerical Techniques in Electromagnetics*, 2nd Ed., CRC Press, 2001.
- [6] C. Bohren, D. Huffman, *Absorption and Scattering of Light by Small Particles*, Wiley, 1983.
- [7] H.Y. Lam, J. Din, L. Luini, A. Panagopoulos, C. Capsoni, "Analysis of Raindrop Size Distribution Characteristics in Malaysia for Rain Attenuation Prediction," 2011 URSI General Assembly and Scientific Symposium, August 2011.
- [8] R. Gunn, G.D. Kinzer, "The terminal velocity of fall for water droplets in stagnant air," *Journal of Meteorology*, Vol. 8, pp.249-253, 1949.
- [9] D.E. Setzer, "Computer transmission through rain at microwave and visible frequencies," *Bell Syst. Tech. J.*, vol. 49, no. 8, Oct. 1970, pp.1873-1892.
- [10] D. Atlas, R.C. Srivastava, R.S. Sekhon, "Doppler radar characteristics of precipitation at vertical incidence," *Rev. Geophys.* Vol. 11, pp.1-35, 1973.
- [11] D. de Wolf, "On the Laws-Parsons distribution of raindrop sizes," *Radio Science*, Vol. 36, No. 4, pp.639-642, July 2001.